DEPARTMENT OF THE ARMY

U.S. ARMY MEDICAL RESEARCH AND MATERIEL COMMAND
FORT DETRICK, MARYLAND 21702-5012

REPLY TO ATTENTION OF
MCMR-RMI-S (70-1y)

ERRATA
AD-B178004

28 Aug 95

MEMORANDUM FOR Administrator, Defense Technical Information Center, ATTN: DTIC-HDS/William Bush, Cameron Station, Building 5, Alexandria, VA 22304-6145

SUBJECT: Request Change in Distribution Statement

1. The U.S. Army Medical Research and Materiel Command has reexamined the need for the limited distribution statement on technical report for Military Interdepartmental Purchase Request Number 92MM2615. Request the limited distribution statement for AD Number ADB178004 be changed to "Approved for public release; distribution unlimited." A copy of this report should be released to the National Technical Information Service.

2. Point of contact for this request is Ms. Judy Pawlus, DSN 343-7322.

for Gary R. Gilbert
GARY R. GILBERT
COL, MS
Deputy Chief of Staff
for Information Management

MIPR NO: 92MM2615

TITLE: ARMY HIGH-PERFORMANCE COMPUTING RESEARCH CENTER FOR THE U.S. ARMY MEDICAL RESEARCH INSTITUTE OF INFECTIOUS DISEASES

PRINCIPAL INVESTIGATOR: Jagdish Chandra
Mark A. Olson

CONTRACTING ORGANIZATION: U.S. Army Research Office
P.O. Box 12211
Research Triangle Park
North Carolina 27709-2211

REPORT DATE: October 1, 1993

TYPE OF REPORT: Final Report

PREPARED FOR: U.S. Army Medical Research and Development Command, Fort Detrick
Frederick, Maryland 21702-5012

REPORT DOCUMENTATION PAGE

Form Approved

1. AGENCY USE ONLY (Leave blank)	2. REPORT DATE	3. REPORT TYPE AND DATES COVERED
	1 October 1993	Final Report (9/28/92-9/30/93)

4. TITLE AND SUBTITLE
Army High-Performance Computing Research Center for the U.S. Army Medical Research Institute of Infectious Diseases

5. FUNDING NUMBERS
MIPR NO. 92MM2615

6. AUTHOR(S)
Jagdish Chandra
Mark A. Olson

7. PERFORMING ORGANIZATION NAME(S) AND ADDRESS(ES)
U.S. Army Research Office
P.O. Box 12211
Research Triangle Park
North Carolina 27709-2211

8. PERFORMING ORGANIZATION REPORT NUMBER

9. SPONSORING/MONITORING AGENCY NAME(S) AND ADDRESS(ES)
U.S. Army Medical Research & Development Command
Fort Detrick
Frederick, Maryland 21702-5012

10. SPONSORING/MONITORING AGENCY REPORT NUMBER

11. SUPPLEMENTARY NOTES

12a. DISTRIBUTION/AVAILABILITY STATEMENT
Distribution authorized to U.S. Government agencies only, Premature Dissemination. Other requests for this document shall be referred to Commander, U.S. Army Medical Research and Development Command, Fort Detrick, Frederick, Maryland 21702-5012. 10Oct93

12b. DISTRIBUTION CODE

13. ABSTRACT (Maximum 200 words)

Molecular-simulation methods in conjunction with X-ray crystallography and interactive computer graphics have been employed for determining key structural and functional features of ligand-bound ricin A-chain. Particular detail has been given to analyzing the structural interactions and energetics governing the binding of two nucleotide ligands, formycin 5'-monophosphate (FMP) and adenyl-3',5'-guanosine (ApG), thought to mimic certain elements of the rRNA substrate. The studies undertaken showed the average simulation structures of the ligand-bound enzyme to be in good accord with the observed X-ray crystal structures in reproducing an overall binding mode. Complementary studies have been carried out aimed at exploring several structural motifs of FMP which would have a greater binding affinity for the active site and perhaps function as template for the development of transition-state analogs for ricin. Building on the binding motif of the adenine ring from the average simulation structures, several substituents have been appended to the base with removal of the ribose and phosphate group leading to the *de novo* design of ligands for ricin.

14. SUBJECT TERMS	15. NUMBER OF PAGES
Ricin; Molecular modeling; Protein structure-based design of enzyme inhibitors, BD, RAD IV	
	16. PRICE CODE

17. SECURITY CLASSIFICATION OF REPORT	18. SECURITY CLASSIFICATION OF THIS PAGE	19. SECURITY CLASSIFICATION OF ABSTRACT	20. LIMITATION OF ABSTRACT
Unclassified	Unclassified	Unclassified	Limited

FOREWORD

Opinions, interpretations, conclusions, and recommendations are those of the author and are not necessarily endorsed by the U.S. Army.

_____Where copyrighted material is quoted, permission has been obtained to use such material.

_____Where material from documents designated for limited distribution is quoted, permission has been obtained to use the material.

_____Citations of commercial organizations and trade names in this report do not constitute an official Department of the Army endorsement or approval of the products or services of these organizations.

_____In conducting research using animals, the investigator(s) adhered to the "Guide for the Care and Use of Laboratory Animals," prepared by the Committee on Care and Use of Laboratory Animals of the Institute of Laboratory Animal Resources, National Research Council (NIH Publication No. 86-23, Revised 1985).

_____For the protection of human subjects, the investigator(s) have adhered to policies of applicable Federal Law 45 CFR 46.

_____In conducting research utilizing recombinant DNA technology, the investigator(s) adhered to current guidelines promulgated by the National Institutes of Health.

_____In the conduct of research utilizing recombinant DNA, the investigator(s) adhered to the NIH Guidelines for Research Involving Recombinant DNA Molecules.

_____In the conduct of research involving hazardous organisms, the investigator(s) adhered to the CDC-NIH Guide for Biosafety in Microbiological and Biomedical Laboratories.

Accesion For	
NTIS CRA&I	☐
DTIC TAB	
Unannounced	
Justification	
By	
Distribution/	
Availability Codes	
Dist	Avail and/or Special
A-1	

Mark A Olson 7-22-93

Principal Investigator's Signature Date

TABLE OF CONTENTS

INTRODUCTION

The function of proteins varies widely in nature as a result of evolution and includes proteins which are toxic to cells. The protein ricin is among the most cytotoxic substances known [1,2]. Ricin functions by inhibiting the synthesis of protein in eukaryotic cells through the hydrolysis of an *N*-glycosidic bond of the adenosine residue in 28S ribosomal RNA (rRNA) [3,4]. Ricin, containing the A- and B-chains, is isolated from the seeds of the castor plant, *Ricinus communis*. The A-chain (RTA) is composed of 267 amino acid residues and contains the enzymatic activity; the B-chain (RTB) is composed of 262 residues and binds to galactose residues present on various cell surface glycoprcteins and glycolipids. Depending on the source of ribosomes and assay conditions, RTA has a K_{cat} and K_m in the range of 300-1500 per min and 0.1-1.3 μM, respectively [5,6]. It has been determined recently that RTA will catalyze the deadenylation of a synthetic GAGA tetraloop oligoribonucleotide with a helical stem of three base-pairs [7]. The nature of the base-pairs does not influence recognition or catalysis by RTA, whereas the position of the tetranucleotide in the loop sequence is critical [7].

In an attempt to elucidate the structural interactions governing the binding of ricin with ribosomes, Monzingo and Robertus [8] have resolved the three-dimensional crystal structures of formycin 5'-monophosphate (FMP) (structure I) and adenyl-3',5'-guanosine (ApG) (structure II) bound in the active site of RTA. Structures were refined at 2.8 Å and 3.0 Å resolution, respectively. These two nucleotide ligands are thought to mimic certain elements of the rRNA substrate, in particular the binding of the

adenine ring. The bound ligands lie perpendicular to a long connecting α-helix near Glu 177 and Arg 180 with the adenine and pyrozolopyrimidine rings stacked between a pair of tyrosines, one from the N-terminus of an adjacent β-strand and the second from an α-helix. The A-chain makes additional contacts through highly polar and charged residues located within joining α-helices linking domains two and three.

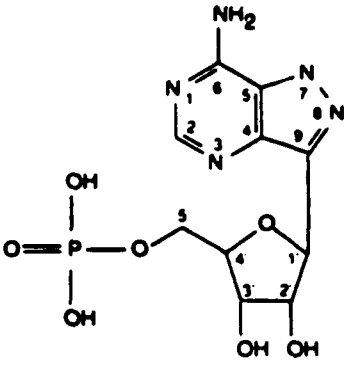

I

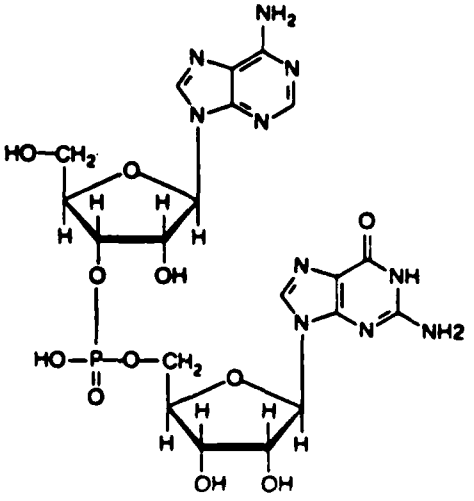

II

To date, no small molecule inhibitors are known for ricin or any of the homologous plant or bacterial toxins. Schramm and coworkers [9,10] have shown FMP to be a powerful transition-state inhibitor of AMP nucleosidase from *Azotobacter vinelandii*, an enzyme that hydrolyses the adenine base from AMP. The tight binding and inhibitory activity of FMP has been attributed to a binding mode of locking the pyrazolopyrimidine ring in a *syn* configuration about its *C*-glycosyl bond [11]. Ricin A-chain recognizes and binds FMP in a *syn* configuration, but is not enzymatically inhibited, and in fact forms a weak binding complex [8].

Analysis by X-ray crystallography suggests that ApG might bind less than FMP [8]. Thus, a knowledge of the structural and energetic determinants of binding ApG versus FMP to the A-chain is clearly important if small nucleotides are to provide a template for successful inhibitor design. Moreover, a detailed understanding of the conformational requisites that binds a GAGA tetraloop to the active site of ricin A-chain is likely to be of great assistance in the development of selective inhibitors. Towards this goal, molecular-dynamics (MD) simulation studies have been performed investigating the binding of FMP, ApG, and the hexanucleotide CGAGAG (data analysis currently in progress) with ricin A-chain. In addition, complementary calculations have been carried out aimed at exploring various structural motifs of FMP which might increase the binding affinity for the active site as well as the *de novo* design of small ricin inhibitors employing FMP as a template.

METHODS, RESULTS AND DISCUSSION

In this section we present the computational methods employed and the results

obtained for the molecular modeling studies outlined above. Discussion of these relative to the goals of the research is presented.

Molecular Modeling Methodology

Molecular-dynamics simulations were carried out using the program DISCOVER [12] with force fields modeled using either AMBER [13] or CVFF [14]. Atomic charges for FMP, ApG, and CGAGAG substrates were determined by either electrostatic potential fitting to a single-point wave function with a 6-31G* basis set using Gaussian 92 [15] or from the AMBER (CVFF) nucleic acid library. Parameters for the protein were taken from the AMBER or CVFF amino acid residue library.

The substrate-bound protein structures were simulated by constructing an active-site region composed of part of the protein and substrate inside a 12-Å spherical boundary as derived from the various crystal structures (FMP and ApG) and from a model docking CGAGAG in the active-site cavity. Amino acid residues lying in the outer shell were fixed at their initial positions and should not introduce significant phase-space sampling errors. Active-site regions for the complexed structures were immersed in a 8-Å deformable layer of water. Water was represented using a flexible SPC potential [16]. Simulations of the various RTA-substrate active regions consisted of: (1) FMP (or analog) plus 63 RTA residues (1026 protein atoms), two sodium counterions, and 362 water molecules; (2) ApG plus 83 residues (1396 atoms), one counterion, and 544 water molecules; and (3) CGAGAG plus 144 residues (2350 atoms), six counterions, and 1231 solvent molecules.

Simulations were initiated with 2000 cycles of minimization using a steepest descent algorithm followed by 30-ps equilibration. The initial atomic velocities were

assigned from a Gaussian distribution corresponding to a temperature of 300 K. Nonbonded interactions were smoothed to zero beyond 9.0 Å and a constant dielectric (ε = 1) was used. All hydrogens were treated explicitly employing a 1.0 fs timestep for integrating the equations of motion. Ensemble averages were determined from a production runs of 100-300 ps with coordinates, velocities, and energies saved every 50 timesteps (0.05 ps) for further analysis. All simulations were carried out on a CRAY Y-MP located at the National Cancer Institute, Frederick Cancer Research and Development Center.

Several structural motifs constructed from the original FMP-bound structure were investigated employing free-energy simulation methods [17]. For estimating the relative binding affinity of FMP and its analogs (denoted as FMP') with the active site of RTA, we make use of the following thermodynamic cycle: $\Delta(\Delta A) = \Delta A_{inhib}' - \Delta A_{inhib} = \Delta A_{bind} - \Delta A_{solv}$, where ΔA_{inhib} and $\Delta A_{inhib}'$ are the Helmholtz free energy of binding for substrates FMP and FMP', respectively; ΔA_{solv} represents the solvation free-energy difference between FMP and FMP', and ΔA_{bind} represents the binding free-energy difference between FMP and FMP' in the RTA active site. Molecular-dynamics simulations were performed for a series of small discrete transformations of FMP into the 2- and 2'-amino and 2-hydroxyl analogs. The force fields were modeled using the CVFF calibrated via MNDO [18] calculations. Simulations of the substrate-bound enzyme employed the active-region methodology as described above. For the

unbound ligand systems, simulations were carried out by placing the solute from the X-ray crystal structure in a cubic box of length 27 Å containing 632 water molecules plus counterions. Periodic boundary conditions were utilized in these latter set of calculations in reducing edge effects.

Free-energy simulation protocol consisted of all systems simulated at ten values of the advancement coordinate λ connecting the initial (crystal structure) state to the mutated state. The λ_1 simulations were initiated with 400 cycles of minimization using a steepest descent algorithm plus 1000 cycles of minimization via a conjugate gradient algorithm followed by 10-ps equilibration. Simulations for λ_2, λ_3, ..., λ_9 were carried out following a 5-ps equilibration started from the final step of the previous simulation. The λ_{10} simulations were initiated with a 10-ps equilibration.

The *de novo* design of ricin inhibitors was performed using a computer program called LUDI [19]. As described in the literature, LUDI can append new substituents onto an already existing ligand (*e.g.*, FMP) in such a way that hydrogen bonds are formed with the protein and hydrophobic pockets are filled with suitable side chains of the ligand. Current efforts are aimed at designing new substituents for the pyrazolopyrimidine ring given the fact that ricin A-chain recognizes both FMP and ApG. Energy refinement of the *de novo* designed complexes were carried out via energy minimization. Poor van der Waals contacts with the protein and poor internal geometries from linking multiple fragments are removed. Measures of the fit and binding of ligands were evaluated through the total nonbonded interaction energies with the receptor.

Results and discussion

Summarized in Table 1 are the averaged intramolecular and nonbonded interaction energies for the RTA-FMP complex computed over 200 ps for the simulation model (AMBER force fields) and the corresponding values for the X-ray structure. The energy contribution that shows significant deviation is the nonbonded electrostatic interactions between RTA and FMP. Superposition of the X-ray structure and simulation structure (shown in Fig. 1) illustrates key structural similarities as well as noticeable differences. In accord with the crystal structure, the simulation structure shows the formycin ring conformationally stacked between the rings of tyrosines 80 and 123. These two residues make strong packing interactions with the substrate stabilizing the binding complex. The hydroxyl group of Tyr 80 further stabilizes the binding of FMP by making several distant electrostatic interactions with the pyrazolopyrimidine moiety and the ribose.

Both the crystal structure and the average simulation structure show FMP strongly interacting with polar groups of the active-site cavity. Most important are several backbone carbonyls that point toward the center of positive charge density of the formycin ring and make hydrogen bonds to its protons. In addition, both structures show N-6 donating a hydrogen bond to the carbonyls of Val 81 and Gly 121, and a hydrogen bond between N-7 and the carbonyl of Gly 121. N-1 is shown to accept a hydrogen bond from the backbone amide group of Val 81.

The average simulation structure is in further agreement with the crystal structure showing FMP interacting with charged residues of the active site, principally Glu 177, Arg 180, and Glu 208. Residues 177 and 180 are located near the C-

terminus of an α-helix which contains a distinct bend allowing the side chains of both residues to reach the molecular surface of the active-site cavity. From the simulation structure the two residues form an ion-pair interaction similar to the interactions observed in the native enzyme crystal structure [20,21,22] and the full MD simulation structure [23]. The guanidinium group of Arg 180 donates a strong hydrogen bond to N-3 of the formycin ring. From the simulation structure the carboxylate of Glu 177 and the backbone carbonyl of Glu 208 make strong electrostatic interactions with the ribose O-2′ and O-3′, respectively. From the X-ray structure the ribose O-2′ appears to be weakly hydrogen bonded to both glutamates.

TABLE 1
COMPARISON OF THE INTRAMOLECULAR AND INTERACTION ENERGIES OF FMP AND APG SUBSTRATES FOR THE X-RAY STRUCTURE AND SIMULATION MODELS

Energy (kcal/mol)	FMP		ApG	
	X-ray[a]	Simulation[b]	X-ray[a]	Simulation[b]
Intramolecular				
angle	51.6	47.6 (0.5)	28.8	47.7 (2.9)
dihedral	11.9	26.0 (3.5)	25.6	29.3 (1.9)
bond	44.8	19.1 (5.7)	5.6	23.5 (2.9)
X-term	0.5	2 6 (0.2)	0.4	0.6 (1.2)
electrostatic	-346.3	-340.9 (2.0)	-465.5	-465.8 (1.7)
van der Waals	7.3	7.2 (2.7)	14.2	14.5 (3.1)
total	-230.2	-238.4 (6.2)	-390.9	-350.2 (11.9)
Interaction				
electrostatic	-68.1	-173.9 (1.8)	-26.0	-139.9 (8.5)
van der Waals	-13.8	-15.3 (1.9)	-15.2	-15.6 (0.2)
total	-81.9	-189.2 (0.1)	-41.2	-155.5 (8.7)

[a] Values for the X-ray structure calculated using partial atomic charges of the corresponding simulation model.
[b] Simulation values listed were averaged over 200 ps for FMP and 300 ps for ApG. the values in parentheses indicate the pertinent standard deviation.

The simulation structure and crystal structure show contributions to the binding of the ligand by the side chain of Ile 172 and amide groups of Asn 122, Trp 211, and Gly 212. Ile 172 packs against the formycin ring and makes a favorable contribution through van der Waals interactions. The amide backbone of residues 122, 211, 212 exert their effect on the binding of FMP primarily through long-range electrostatic interactions with N-7 for residue 122, and both the ribose O-3' and phosphate group for residues 211 and 212.

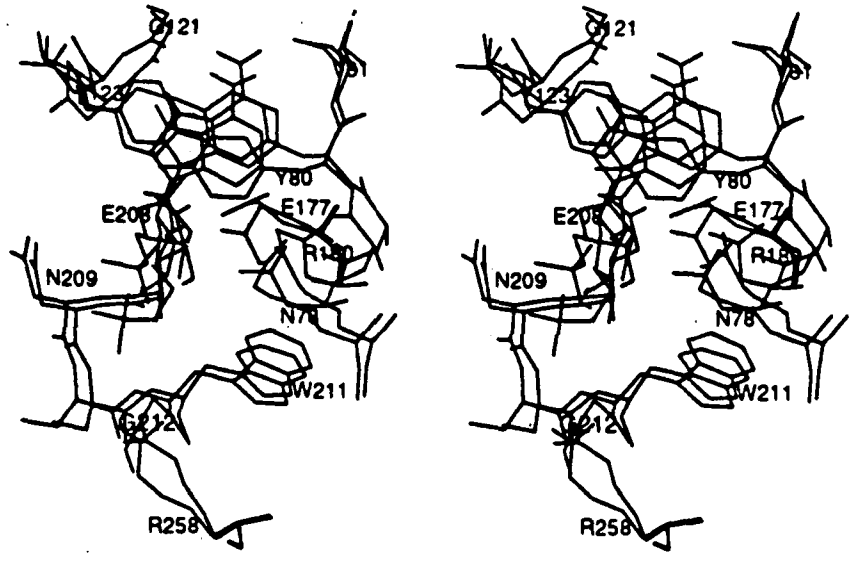

Figure 1. Stereoview overlay showing a superposition of the average simulation structure and X-ray crystal structure for the binding RTA-FMP complex.

Structural differences between the X-ray crystal structure and the average simulation structure for the molecular model system are derived primarily from interactions between the phosphate group and protein atoms. From the X-ray

structure the phosphate group projects out of the binding pocket into the solvent and makes a long-range (4.7 Å) electrostatic interaction with the positively charged guanidinium group of Arg 258. The average simulation structure shows the phosphate group at a lower position as a result of strong ion-pair interactions with Arg 258 and long-range interactions with Arg 180. Nonbonded interaction energy for residue 258 corresponding to the simulation structure is approximately two-fold greater than the crystal structure.

The average simulation structure shows the phosphate group strongly interacting with eight water molecules, three of which are bridge forming waters with side chains of Tyr 80, Gly 212, and Arg 258. Because of strong electrostatic interactions of the phosphate group with protein atoms, the simulation structure suggests a less restrictive solvent accessible surface area for the ribose than observed in crystal structure showing two possible hydrogen bonds with water molecules, one bridging Gly 212 and the phosphate group. The simulation also clearly shows the desolvation of several key active-site residues upon binding of FMP. A comparison of the RTA-FMP simulation structure with the average MD simulation structure of the native enzyme shows the loss of approximately five water molecules bound to residues Glu 177, Arg 180, and Glu 208. These waters are thought to be critical nucleophiles in the development of a transition-state like binding complex of the ribosome [8,20,23].

Examination of the structures of FMP in the RTA active site during the 200-ps molecular-dynamics simulation shows noticeable thermal fluctuations in the phosphate backbone and formycin ring while the sugar remained relatively rigid along

the ribose O-4′ backbone and somewhat flexible in the hydroxyl groups.

TABLE 2
COMPARISON OF X-RAY AND COMPUTED TORSION ANGLES FOR FMP IN THE RTA ACTIVE SITE

Torsion angle[a]	X-ray	Simulation
α	166.2	169.2 (6.3)[b]
β	-173.9	88.8 (8.1)
γ	-70.1	-110.6 (5.4)
δ	75.2	86.1 (5.0)
θ_0	44.1	42.1 (3.7)
θ_1	-40.4	-33.0 (4.8)
θ_2	21.5	12.5 (6.4)
θ_3	6.5	13.8(5.9)
θ_4	-31.2	-35.2 (4.4)
χ	128.1	113.2 (5.9)

[a] Employing IUPAC nomenclature for backbone torsion angles, ribose endocyclic torsions, and glycosidic torsion.
[b] Values in parentheses indicate the pertinent standard deviation.

Table 2 lists a comparison of the torsion angles describing the conformation of FMP obtained from the X-ray structure and the average simulation structure. The calculated backbone torsion angles β and γ show deviations from the crystal structure of about 94° and 41°, respectively, and can be attributed to the significant interactions between protein atoms and the phosphate group of the simulation model. The simulation structure shows exocyclic and endocyclic torsions corresponding to a 3′-*endo* pucker in agreement with the conformation observed in the crystal structure.

Calculated endocyclic torsions appear to be driven by interactions of the ribose ring with glutamates 177 and 208. From the crystal structure the formycin ring shows a high *syn* configuration with a torsion χ of about 128° and the simulation model shows χ having a value near 113° ± 6°.

Several structural motifs constructed from the original FMP structure were investigated using free-energy simulation methods for the dianion and monoanion models. For the 2-amino formycin 5′-phosphate analog transformation, the free energies calculated for the enzyme-bound ligand (ΔA_{bind}) predict the analog to interact more favorably with the enzyme in both dianion and monoanion simulation models. However, the *relative* binding free energies ($\Delta\Delta A$) predict the 2-amino analog to bind less strongly to RTA than does FMP itself. Selectivity reflects solvation effects, as it is less difficult to desolvate FMP than its 2-amino derivative. The lack of significant sensitivity in the relative free-energy change on the ionization state of the phosphate group suggests a dominate van der Waals component contribution to $\Delta\Delta A$.

Of the free-energy simulations for the 2-hydroxyl formycin 5′-phosphate analog, the monoanion model shows a greater relative binding affinity ($\Delta\Delta A$ =-1.8 kcal/mol) for the active site of RTA than the original FMP substrate. Analysis of the average end-point structure shows several changes in the structural interactions between the ligand and residues Tyr 80, Glu 177, and Arg 180. Most important, the carboxylate of 177 interacts favorably with the hydroxyl group. The formycin ring of the hydroxyl analog

appears to be a high *syn* conformation (χ= 150°) and makes several strong interactions found in the FMP simulation structure, most notably interactions with the polar backbone of Val 81 and Gly 121 as well as packing interactions with Tyr 80 and Tyr 123. Finally, decomposition of $\Delta\Delta A$ shows a large electrostatic free-energy interaction component dominating the improved binding of the ligand.

As for the 2′-amino formycin 5′-phosphate analog, neither of the two simulation models predict a relative increase in binding affinity for the enzyme. Both ΔA_{bind} and ΔA_{solv} show a decrease in favorable interactions with the enzyme and solvent, respectively.

Molecular-dynamics simulation of the structural interactions governing the binding of ApG with the active of RTA was carried out for 300 ps. Summarized in Table 1 are the averaged intramolecular and interaction energies for ApG in the ricin A-chain active site computed from the simulation and the corresponding values determined from the crystal structure. Energies are partitioned into covalent, electrostatic, and van der Waals terms in accord with the form of the AMBER potential function. The energy contributions that show significant deviations are the angle and bond strain terms as well as the electrostatic interaction binding term. Figure 2 shows a superposition of the average simulation structure and X-ray crystal structure. The root-mean-square (RMS) deviation for the enzyme-substrate complex is roughly 0.66 Å and a fit of the substrate structures yields 1.21 Å. From the crystal structure, the adenine ring is conformationally stacked between the rings of tyrosines 80 and 123

Both residues provide efficient packing interactions stabilizing adenine binding. In addition, both tyrosines stabilize the binding of the guanosine ribose by making several long-range electrostatic interactions and van der Waals contacts. Comparable hydrophobic contacts are found in the average simulation structure, however, the substrate conformation is shifted by approximately 1 to 3 Å with the largest Cartesian coordinate differences occurring in the adenine and guanine rings. This shift is driven in part by a strong hydrogen bond between the amide backbone of Tyr 123 and N-7 of adenine. The crystal structure shows no strong enzyme ion-pair interactions with the imidazole ring; the amide backbone of Tyr 123 is at a distance of 3.62 Å and functions to secure both hydroxyl groups on the guanosine ribose. The width of the adenine binding slot, as measured from the distance between the centroids of the tyrosine rings, is about 9.93 Å in the simulation structure versus 8.86 Å in the crystal structure, and 9.15 Å in the substrate-free A-chain crystal structure [20]. Centroids measured from the pyrimidine ring to the tyrosine rings in the simulation structure are 5.49 Å and 5.25 Å for tyrosines 80 and 123, respectively, and 3.77 Å and 6.15 Å, respectively, in the crystal structure. The packing arrangement of the tyrosines with the adenine ring in the simulation model exhibits greater edge-to-face interactions characteristic of aromatic-aromatic interactions in proteins described by Burley and Petsko [24]. A comparison of rotameric states for residues 80 and 123 in the average simulation structure and crystal structure finds noticeable variances. For Tyr 80, χ_1 = (-145°, simulation; -153°, X-ray) and χ_2 = (-132°, simulation; 82°, X-ray), and for Tyr 123, χ_1 = (-155°, simulation; -81°, X-ray) and χ_2 = (-64°, simulation; 59°, X-ray). It is important to

note that tne side-chain of Tyr 80 undergoes several structural transitions, as discussed further below. In spite of differences in orientation, the net contribution of the two tyrosines to the total van der Waals interaction energies binding the adenine ring is calculated to be about -4 kcal/mol in both the simulation structure and the crystal structure.

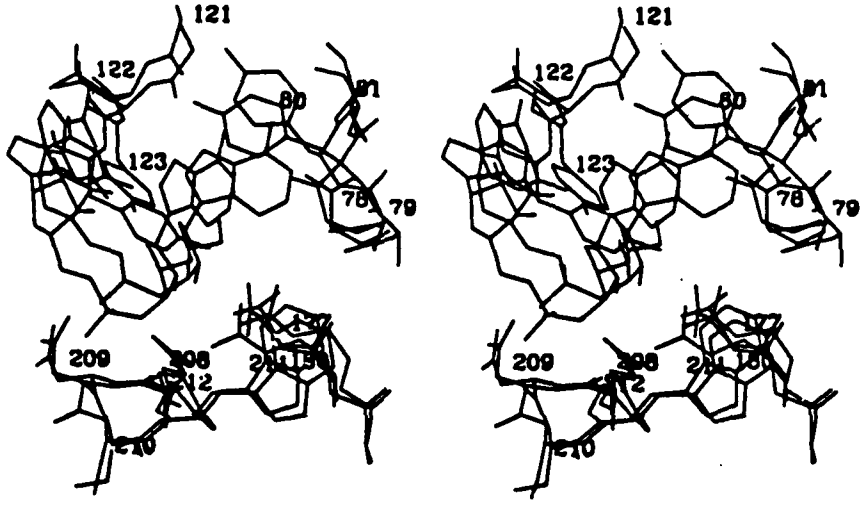

Figure 2.Stereoview showing a superposition of the average simulation structure and X-ray crystal structure for the binding RTA-ApG complex.

In addition to the hydrogen bond between N-7 and Tyr 123, the average simulation structure shows the adenine ring partially "solvated" by ion-pair interactions between the protons at N-6 and the backbone carbonyls of Val 81 and Gly 121. The crystal structure shows similar interactions for N-6 plus a strong hydrogen bond between N-1 and the amide group of Val 81 (2.49 Å versus 4.64 Å in the simulation). The significance of these substrate-protein interactions with the polar backbone of

residues 81 and 121 is that they conceivably provide the hydrogen-bonding pattern that specifically recognizes bases in the order ApG versus GpA, which has been shown not bind to the A-chain [8]. Examination of the dihedral angles ϕ and ψ for Val 81 shows the simulation structure located in the same region of conformational space as the crystal structure placing the residue at (-45°,76°) compared with (-56°,88°). In contrast, Gly 121 in the X-ray crystal structure exhibits dihedral angles of (-62°,-97°), while the simulation samples the conformation (60°,-119°). From the free enzyme crystal structure [20], Gly 121 adopts the conformation (-82°,-6°) and contains a hydrogen bond between the carbonyl and the hydroxyl of Tyr 80. This hydrogen bond is replaced by substrate interactions with the net effect of Val 81 and Gly 121 stabilizing binding by -3 kcal/mol (-2 kcal/mol electrostatic) in the simulation structure and -4 kcal/mol (-2 kcal/mol electrostatic) in the crystal structure.

Substrate binding in the simulation structure and the crystal structure is significantly stabilized by the guanidinium group of Arg 180 which forms several ion-pair interactions, one of which is a key hydrogen bond with N-3 of the adenine ring. The simulation structure predicts a distance of about 2.85 Å between the guanidinium group and N-3 compared with 2.55 Å observed in the crystal structure. Mutagenic studies have implicated Arg 180 as the principal catalytic residue. The conversion of Arg 180 to a lysine showed minor effect on enzyme activity, while the conversion to a histidine resulted in a 1000-fold reduction in activity [25]. From a mechanistic viewpoint, Arg 180 together with a water molecule is thought to be critical for protonating adenine at N-3 in facilitating bond breakage during deadenylation of the rRNA substrate [8,20]. Both the average simulation structure and the crystal structure

show the substrate-bound active site lacking a water positioned near Arg 180. Though the refined crystal structures of RTA and the recombinant A-chain exhibits a trapped water bound to the guanidinium group and Glu 177 [20,22]. The crystallographic thermal factor for this water is roughly 8 Å^2 [20] and reflects its thermodynamic stability in the structure of the active site. The loss in solvent contribution to stabilizing substrate interactions with Arg 180 is compensated by the formation of ion-pair interactions between the positively charged guanidinium group and the adenosine ribose O-2′ together with favorable long-range electrostatic interactions with the guanosine and phosphate group. There appears to be little difference in the orientation of the Arg side chain in the free and substrate-bound structures (simulation and X-ray), both showing a (−,t) rotameric state. Likewise, there is little difference in solvent accessible surface area. The simulation predicts for Arg 180 a total interaction energy with ApG of roughly -38 kcal/mol and the crystal structure yields -31 kcal/mol. Energetic differences are derived primarily from the phosphoryl and guanosine ribose interactions. Decomposition of the Arg 180 structural interaction energies in terms of substrate functional groups for the simulation structure finds -11 kcal/mol interaction with the adenine ring, -16 kcal/mol with the adenosine ribose, -9 kcal/mol with the phosphoryl group, and -2 kcal/mol for the guanosine ribose structure.

The highly conserved residue Glu 177 has been proposed to stabilize the transition-state oxycarbonium ion on adenosine in the ribosome substrate [8]. Analysis of the conformation of ApG from both the crystal structure and the average simulation structure shows the adenine ring in a high *syn* configuration (discussed further below) lacking the required orientation to mimic cation stabilization on the

ribose by Glu 177. From the crystal structure the carboxylate shows a hydrogen bond with the adenosine O-2', while the simulation structure shows no direct ion-pa. interactions with the substrate, but contains a strong hydrogen bond with Arg 180 as was found in the free enzyme [20]. Although Glu 177 is an important residue in the enzyme activity of the A-chain [26], an examination of the interaction energies of both structures suggests a net *destabilizing* contribution to the binding of ApG by the carboxylate primarily through poor interactions with adenosine ribose in the simulation structure, and the adenine ring and guanosine ribose in the crystal structure. Presumably the carboxylate plays a key role in anchoring Arg 180 for substrate binding and catalysis as well as maintaining the structural integrity of the active site. Recent molecular-dynamics simulations of point mutations Glu 177 to Gln and Ala in the native ricin A-chain indicates significant destabilizing free-energy electrostatic interactions arising from the guanidinium group of Arg 180 in the mutant folded proteins [27].

Other key residues making favorable substrate binding interactions in the average simulation structure include Glu 127, Arg 134, and Arg 213. Of these residues, only Arg 134 contributes to substrate binding in the crystal structure. The carboxylate of Glu 127 lies near the C terminus of an α-helix and appears to stabilize the binding of the guanosine ribose through long-range electrostatic interactions with the hydroxyl groups (calculated to be about -5 kcal/mol). The side chain of the highly conserved residue Arg 134 is located within a large solvent exposed coil running along the active-site cleft and makes several favorable electrostatic interactions w.

the substrate; the adenine ring (-8 kcal/mol, simulation; -2 kcal/mol, X-ray), both ribose structures (-20 kcal/mol, simulation; -12 kcal/mol, X-ray), and the phosphate group (-12 kcal/mol in both simulation and X-ray). Similar strong electrostatic interactions are observed for Arg 213 in the simulation structure with the phosphate backbone (-11 kcal/mol) and the guanosine ribose (-12 kcal/mol), both of which are lacking in the crystal structure. The guanidinium group of Arg 213 projects out from an α-helix with a predicted (−,+) rotamer conformation, while the crystal structure shows a (−,t) conformation with the residue exposed more towards the solvent but less than in the free A-chain crystal structure [20]. Collectively these predicted protein-substrate interactions for arginines 134 and 213 in the simulation model of the RTA-ApG complex contribute -63 kcal/mol toward stabilizing substrate binding and may conceivably mimic certain individual recognition points for the RNA stem and loop residues flanking the adenine ring, although Arg 213 is poorly conserved in the *N*-glycosidase toxin family. Monzingo and Robertus [8] have constructed several theoretical models binding the hexanucleotide sequence CGAGAG with the active site of ricin A-chain employing the NMR defined ···CGAAA··· hairpin sequence determined by Heus and Pardi [28]. From their models, both arginines appear to display ion-pair interactions which are characteristic of the type of structural elements found in the ApG-bound RTA simulation structure. In one of their models, Arg 134 ion-pairs with the phosphate backbones of G2 and A3 (the target of deadenylation), and Arg 213 pairs with the phosphate of C1. Further stabilizing interactions are found for Arg 258 with the G5 phosphate backbone.

The simulation structure is in agreement with the crystal structure showing two

hydrogen bonds between the guanosine moiety and residues Asp 124 and Asn 209. The amide backbone of Asp 124 makes an ion-pair interaction with the ribose O-2' (2.03 Å, simulation; 2.02 Å, X-ray) and the side-chain amide nitrogen of conserved Asn 209 donates a hydrogen bond to a phosphoryl oxygen (1.81 Å, simulation; 2.61 Å, X-ray). The simulation structure predicts, however, a net 12 kcal/mol greater binding stabilization for both residues than observed in the crystal structure. Additional protein interactions with the substrate are formed by the conserved residue Ile 172 and the invariant residue Trp 211. The side chains of 172 and 211 make favorable hydrophobic interactions with the adenine and adenosine ribose, respectively. The indole ring lies parallel and provides addition anchoring support for the side chain of Arg 180. Chemical modifications of Asn 209 to a Ser and Trp 211 to a Phe have been shown to produce little effect on the depurination of the ribosome [26] suggesting involvement in base recognition or related functions.

Binding differences between the average simulation structure and the crystal structure can be further characterized from analyzing the substrate solvent accessible surface area and molecular volume. The crystal structure shows the substrate more exposed to solvent with a 25 $Å^2$ greater surface area (employing a 1.4 Å radius spherical probe) and a 300 $Å^3$ greater molecular volume. Taken together, the contraction of the average simulation substrate structure at protein surface is consistent with stronger binding interactions. The simulation model shows the substrate interacting with five water molecules. The diffusion coefficient of the bound waters calculated using the Einstein relation is roughly 0.14 $Å^2 \cdot ps^{-1}$, compared with

0.70 $Å^2 \cdot ps^{-1}$ for all the waters in the simulation system. Two of the bound waters are bridge-forming waters with guanosine and protein side chains; one bridging O-5′ and Arg 213, and the second bridging HO3′ with residues Asp 124 and Arg 134. One of the waters appears to be bound by the substrate in a four-sided negatively charged density region composed of N-3, O-4′, O-5′ of guanosine and O-4′ of adenosine. The remaining waters are hydrogen bonded to protons at N-1 and N-2 of the guanosine.

As shown in Table I, the X-ray crystal structure and the average simulation structure are comparable in total intramolecular electrostatic energies. The crystal structure shows a strong intramolecular hydrogen bond between HO-3′ of the guanosine ribose and a phosphoryl oxygen. Weaker hydrogen bonds may be formed between HO-3′ and either O-4′ of adenosine or O-5′ of guanosine. The simulation structure contains two hydrogen bonds; a strong hydrogen bond between the hydroxyl group of the adenosine ribose and a phosphoryl oxygen plus a second weaker bond between O-5′ of adenosine and a proton at N-2 of the guanine ring. The simulation showed little variation in the bond common to the hydroxyl group (1.7 ± 0.1 Å), whereas the adenosine-guanine hydrogen bond appears to be less stiff (2.5 ± 0.3 Å). For comparison purposes the intramolecular distances between C-5′ and N-9 for both nucleotides as a function simulation time have been computed. The simulation predicts averaged distances of 3.9 ± 0.4 Å and 4.8 ± 0.1 Å for adenosine and guanosine, respectively, versus 3.9 Å and 4.3 Å, respectively, for the crystal structure.

The simulation shows a transition of about 1 Å in the adenosine C-5′-N-9 distance which may be facilitated in part by a short-lived conformational transition in the ribose (discussed further below). The average RMS fluctuation for ApG calculated for the heavy-atoms is about 0.48 Å compared with 1.33 Å estimated from the crystallographic thermal factors of the refined structure [8]. The guanosine base and ribose showed the largest thermal fluctuations consistent with lower binding interaction energies.

A comparison of the torsion and pseudorotation angles describing the substrate conformation obtained from the X-ray crystal structure and the average simulation structure is listed in Table 3. The backbone torsional angles α and ß predicted by the simulation show deviations from the crystal structure of about 30° and 94°, respectively, and can be attributed to differences in electrostatic interactions between the phosphate group and arginines 134 and 213 as well as intramolecular hydrogen bonds. The calculated dihedral angles γ and δ for adenosine are in good accord with the crystal structure, whereas the simulation predicts a different conformation for guanosine. Similarly, the predicted endocyclic torsions of the adenosine ribose compares well against the crystal structure, unlike most guanosine values. Both the average simulation structure and the crystal structure exhibit *syn* base configurations for the adenine and guanine rings, however the conformations differ by roughly 57°.

Analysis of the crystal structure shows C3′-*exo* and C3′-*endo* ribose pucker configurations for adenosine and guanosine, respectively. The simulation model indicates that the adenosine ribose is in a dynamic equilibrium consisting of C3′-*exo*

and C2′-*endo* configurations. Short-lived dihedral transitions to a C1′-*exo* configuration occurred during the simulation. The greatest fluctuations were found in dihedrals θ_1, θ_2, and θ_3 for adenosine. The adenine ring exhibited a glycosidic torsion fluctuation of about 50° at the latter transition, but remained in *syn* configuration. No transitions occurred for guanosine, which showed a C4′-*exo* pucker configuration throughout the simulation.

TABLE 3
COMPARISON OF X-RAY AND COMPUTED TORSION ANGLES FOR ApG IN THE RTA ACTIVE SITE

Torsion angle	X-ray		Simulation	
	A	G	A	G
α		-158.0		-187.7 (8.7)
β		-81.1		-175.0 (13.3)
γ	-168.4	-47.6	-175.3 (13.3)	41.8 (10.2)
δ	144.2	81.4	144.1 (8.8)	65.4 (5.8)
θ_0	-33.1	43.3	-32.6 (4.1)	23.1 (5.4)
θ_1	33.5	-42.5	30.0 (19.9)	-40.1 (4.6)
θ_2	33.5	24.5	-22.5 (10.6)	42.0 (5.1)
θ_3	-1.4	4.5	0.9 (10.1)	-27.2 (6.4)
θ_4	22.5	-31.5	20.5 (6.1)	1.2 (6.5)
χ	94.2	15.5	150.8 (10.3)	73.4 (9.3)
P	196.6	13.1	198.2	57.2

[a] Values in parentheses indicate the pertinent standard deviation.

To further characterize the conformational dynamics of ApG in the active site of the A-chain, side-chain and backbone dihedral angles of several key residues were examined as a function of simulation time. The side chains of Tyr 80 and Arg 180

showed significant dihedral angle changes which were greater than the fluctuations of the angle. Of these residues, Tyr 80 clearly showed angle changes which directly influence and/or accommodate the conformational changes in the bound substrate. Structurally, Tyr 80 is the initial residue in an antiparallel ß-sheet following a reverse turn, and as shown above, provides a thermodynamically stable, hydrophobic environment for the substrate. Relative to the X-ray crystal structure of the free enzyme [20], Tyr 80 is the only residue which shows any appreciable conformational change upon binding ApG. The crystallographic dihedral angles (χ_1,χ_2) are displaced from (-151°,-86°) to (-153°,80°). Initially from the trajectories, χ_1 and χ_2 are located at (-86°,-130°). At 25 ps χ_1 is displaced and oscillates around a slightly different value from the initial equilibrated conformation, yet the side chain remains within the same rotameric state. This subtle change appears to be in response to the 60° or greater increase in θ_1 of the adenosine ribose. The trajectories showed Tyr 80 underwent large angle excursions at roughly 50 ps through 100 ps, at 165 ps, 210 ps, and 275 ps. Fluctuations starting at 90 ps results in a transient packing defect leading to the transition at 100 ps with the potential minima located at (-175°,-116°). The transition at 165 ps correlates with the short-lived C1′-*exo* repuckering in the adenosine ribose coupled with the fluctuations in the adenine glycosidic torsion. There are two additional transitions at about 210 ps and 275 ps. The former transition is due to the replacement of a hydrogen bond between the backbone carbonyl of Tyr 80 and the backbone amide of Asp 75 with a bond between the carbonyl and the amine group of

the adenine ring. The average dynamic structure shows a CO-HN (adenine) distance of 4.62 Å, as compared with 4.35 Å from the X-ray crystal structure. The latter transition in χ_2 corresponds to fluctuations in the hydrogen-bonding pattern of the side-chain atoms for Asp 75 and Asn 78.

The simulation predicts several structural transitions in the backbone angles of Tyr 80 which are correlated with the calculated fluctuations in adenosine outlined above. From 0 to 50 ps, (ϕ,ψ) has oscillations near (-52°,114°), which represents the observed crystallographic conformation. This state is followed by large fluctuations up to 100 ps leading to the second state where (ϕ,ψ) has oscillations at (19°,81°), and is interrupted by the short-lived transition state at 165 ps with oscillations near (-128°,130°). The fourth state has oscillations at (53°,-43°), remaining throughout the simulation. No similar transitions were found in the simulation for Tyr 123 or any other active-site residue nor were there any comparable transitions found in the MD simulation of the free enzyme [23]. Thus, suggesting Tyr 80 may function as the key determinant of substrate modulation and orientation in the active site once recognition has occurred, principally by arginines 134, 180, and 213. Relative to the free enzyme simulations [23], the magnitudes of the side-chain and main-chain positional RMS fluctuations for Tyr 80 in the bound simulation are significantly altered. There also appears to be substrate effects on the dynamics of Asp 75 plus reverse-turn residues 76-79. The main-chain and side-chain fluctuations of these residues change by as much as 0.2-0.4 Å between the free and bound simulations. The free enzyme structure comprises of a reverse-turn hydrogen bond between HN of Asn 78 and the

carbonyl of Asp 75 together with a ß-sheet bond between the carbonyl of Tyr 80 and HN of Asp 75. As shown above, this latter ion-pair interaction switches during the bound simulation to pair with the adenine ring. The average simulation structure exhibits several ion-pair interactions between Asn 78 and various residues within the reverse-turn and ß-sheets; the backbone carbonyl of Asn 78 pairs with the amide group of Tyr 80; the carboxylate of Asp 75 pairs with the nitrogen side-chain of Asn 78 plus the amide group of Thr 77; and the amide backbone groups of Asn 78 and Ala 79 pair with the carbonyl of Asp 75. The X-ray crystal structure of the bound-state shows similar hydrogen bonds with the notable exception of forming an alternative ion-pair interaction between the amide group of Tyr 80 and the side-chain oxygen of Asn 78. These additional reverse-turn interactions observed in the bound-state structures appear to be stabilized by the binding of ApG. It is reasonable that this structural element corresponding to residues 75-80 could play an important entropic role in binding substrates.

The dihedrals of Arg 180 showed large fluctuations near 135 ps, but remained in a (–,t) rotameric state. Fluctuations were of a jump-and-return nature and appear to be due primarily to shifts in hydrophobic interactions with Glu 177 and Trp 211. There were no corresponding fluctuations in the backbone angles for Arg 180. For arginines 134 and 213, the trajectories exhibited no fluctuations in 134 and only minor side-chain displacements in 213, which were correlated with the adenosine phosphate backbone γ displacements. Comparisons with the free enzyme simulation, arginines 134, 180, and 213 showed decreased positional fluctuations in the bound-state simulation. The loss of flexibility in these key residues in the presence of ApG is

readily understood in terms of specific enzyme-substrate interactions outlined above.

It is of interest to compare the binding of ApG with that of FMP. As mentioned in the Introduction, analysis by X-ray crystallography suggests that ricin A-chain has a binding preference for FMP [8]. An examination of the binding motifs of the adenine and pyroazolopyrimidine rings in the two substrates shows similarity in packing and ion-pair formation, however there are several positional and conformational shifts. These adjustments correspond primarily to the pyroazolopyrimidine ring able to form an extra hydrogen bond to the polar backbone of the active site coupled with fewer electrostatic and orientation constraints of the phosphate backbone in FMP. A comparison of the total binding interaction energies calculated from the MD simulation of the RTA-FMP complex with the simulation of the RTA-ApG complex indicates a difference of about 40 kcal/mol, favoring FMP binding. Both simulations predict significantly greater binding interactions than observed in the crystal structures. Differences in structural interactions between the two substrates are primarily electrostatic in origin as hydrophobic contacts are roughly equal. The average simulation structure of the ApG complex contains less efficient electrostatic binding interactions, principally those of the dinucleotide phosphoryl group and adenosine. When combined with the guanosine ribose, the two ribose structures of ApG approximate the FMP ribose-protein interactions. Key residues which make significant contributions to the binding of FMP but not ApG include Asp 124, Glu 208, Gly 212, and Arg 258. The first two residues make favorable electrostatic interactions with the ribose group; the backbone carbonyl of 208 forms a strong hydrogen bond. The amide backbone of Gly 212 and Trp 211 together with the guanidinium group of Arg

258 (which substitutes for Arg 213 in the ApG binding mode) provides partial neutralization of the negative charge of the phosphoryl group. As in the binding of ApG, Arg 180 makes significant stabilizing interactions securing FMP in the active site and forms a strong ion-pair interaction with N-3. The carboxylate of Glu 177 makes favorable binding electrostatic interactions with the ribose (unlike that of ApG), but poor interactions with the pyroazolopyrimidine ring.

Building on the average simulation structures for substrates FMP and ApG bound in the RTA active site, design studies are being carried out aimed at determining new ligands with improved binding. Current efforts are directed at appending new substituents onto the existing FMP and ApG structures. Shown below (structure III) and in Figure 3 is an example of a proposed ligand structure constructed from molecular-dynamics simulations of the adenine-like ring in FMP bound to the active site of RTA.

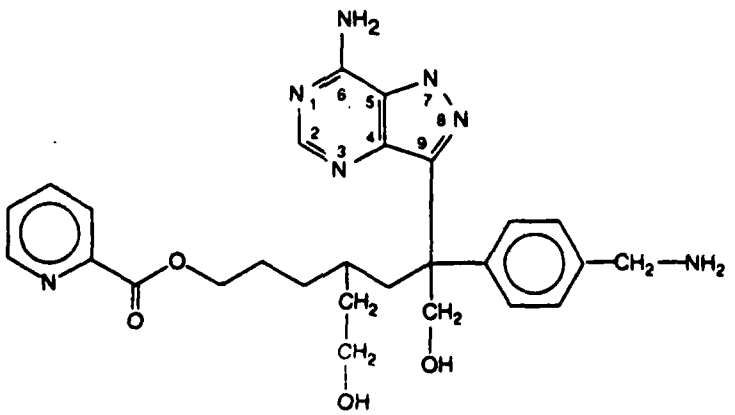

III

This structure seems promising in that the proposed ligand does not contain a highly charged phosphate group as compared with FMP, while having approximately the same interaction energy with the protein.

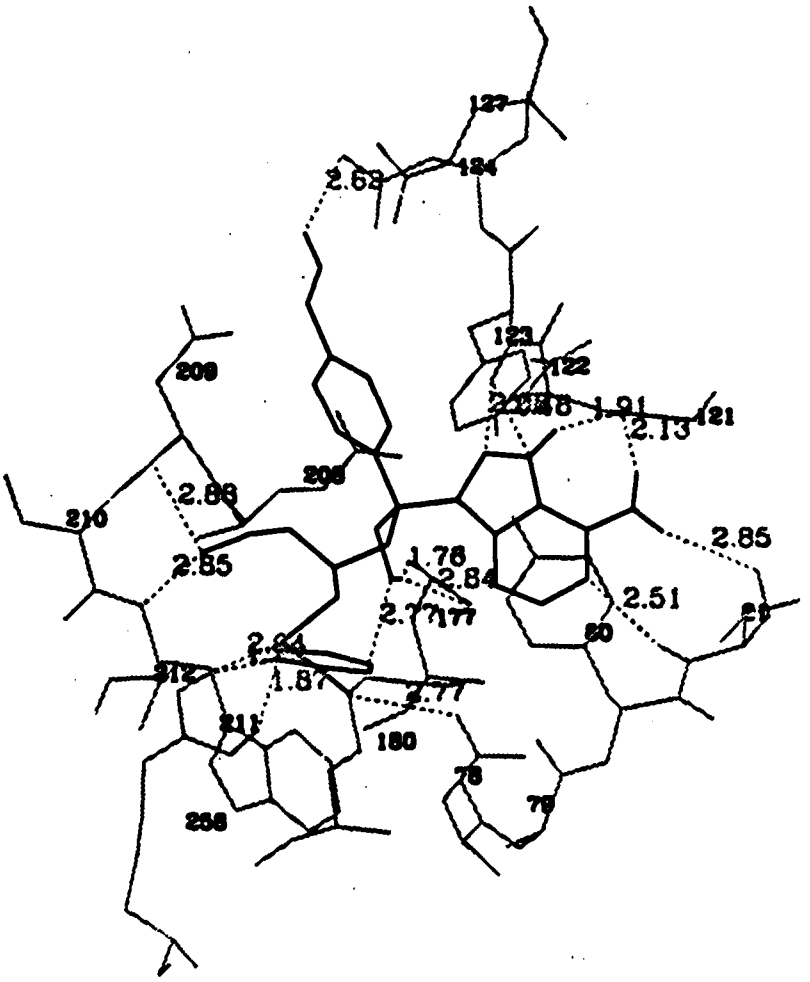

Figure 3. *De Novo* ligand design. Structure **III** in the active site of ricin A-chain.

CONCLUSIONS

Ricin A-chain is a cytotoxic protein that attacks ribosomes by hydrolyzing the adenine ring from a specific adenosine, thereby inhibiting protein synthesis. The substrate binding complexes of formycin 5′-monophosphate and adenyl-3′,5′-guanosine in the ricin A-chain active site were investigated by molecular-dynamics simulations immersed in solvent water. The studies undertaken showed the average simulation structures of the substrate-bound enzyme to be in good accord with the observed X-ray crystal structures in reproducing overall binding modes. However, there are significant differences in the location and binding of various substrate functional groups. For FMP, the simulation predicts significant differences in the location and binding of the phosphate group. For ApG, the calculated average structure of the bound substrate is shifted 1 to 3 Å from the X-ray structure, while retaining a similar binding motif for adenosine. The simulation predicts greater protein-ApG binding interactions, particularly among the guanosine ribose and phosphoryl function groups. Free-energy simulation methods have been employed to explore several structural motifs of FMP which would have a greater binding affinity for the active site. It is shown that ricin A-chain has a preference for FMP over analogs 2- and 2′-amino formycin 5′-phosphate and 2-hydroxyl formycin 5′-phosphate. Using the binding motif of the adenine ring from the average simulation structures, several substituents have been appended to the base with the removal of the ribose and phosphate group leading to the design of new ligands for ricin. These potential antidotes are being further evaluated by molecular-dynamics simulations to determine the relative binding affinities.

REFERENCES

[1] Eiklid, K., Olsnes, S & Pihl, A. (1980) *Expt. Cell Res.* **126**, 321.

[2] Olsnes, S. & Pihl, A. (1982) In *Molecular Action of Toxins and Virsuses* (Cohen, P. & van Heyningen, S., eds), pp.51-105, Elsevier Biomedical Press, New York.

[3] Endo, Y. & Tsurugi, K. (1987) *J. Biol. Chem.* **262**, 8128.

[4] Endo, Y., Mitsui, K., Motizuki, M. & Tsurugi, K. (1987) *J. Biol. Chem.* **262**, 5908.

[5] Olsnes, S., Fernadez-Puentes, C., Carrasco, L., & Vasquez, D. (1975) *Eur. J. Biochem.* **60**, 281.

[6] Ready, M.P., Kim, Y., & Robertus, J.D. (1991) *Proteins* **10**, 270.

[7] Glück, A., Endo, Y., & Wool, I.G. (1992) *J. Mol. Biol.* **226**, 411.

[8] Monzingo, A.F. & Robertus, J.D. (1992) *J. Mol. Biol.* **227**, 1136.

[9] DeWolf, W.E., Jr, Fullin, F.A., & Schramm, V.L. (1979) *J. Biol. Chem.* **254**, 10868.

[10] Leung, H.B. & Schramm, V.L. (1980) *Biochemistry* **255**, 10867.

[11] Giranda, V.L, Berman, H.M., & Schramm, V.L. (1988) *Biochemistry* **27**, 5813.

[12] Biosym Technologies, Inc., San Diego, CA.

[13] Weiner, S.J., Kollman, P.A., Nguyen, D.T., & Case, D.A. (1986) *J. Comp. Chem.* **7**, 230-252.

[14] Dauber-Osguthorpe, P., Roberts, V.A., Osguthorpe, D.J., Wolff, J, Genest, M., & Hagler, A.T. (1988) *Proteins* , **4**, 31.

[15] Gaussian, Inc., Pittsburgh, PA.

[16] Teleman, O., Jönsson, B., & Engström, S. (1987) *Mol. Phys.* **60**, 193.

[17] van Gunsteren, W.F. & Weiner, P.K. (ed.) *Computer Simulation of Biomolecular Ststems.* ESCOM. Leiden, (1989).

[18] Stewart, J.J.P . MOPAC 5.0, QCPE, (1989) *QCPE Bull.*, **9**, 123.

[19] Böhm, J.H. (1992) *J. Comput. -Aided Mol. Design* **6**, 69.

[20] Katzin, B.J., Collins, E.J., & Robertus, J.D. (1991) *Proteins* ,**10**, 251.

[21] Rutenber, E., Katzin, B.J., Collins, E.J., Misna, D., Ernst, S.E., Ready, M.P., & Robertus, J.D. (1991) *Proteins*, **10**, 240.

[22] Misna, D., Monzingo, A. F., Katzin, B. J., Ernst, S., & Robertus, J. D. (1993) *Protein Science* **2**, 429.

[23] Olson, M.A. (manuscript in preparation).

[24] Burley, S. K. & Petsko, G. A. (1985)*Science 229*, 23.

[25] Frankel, A., Welsh, P., Richardson, J., & Robertus, J.D. (1990) *Mol. Cell. Biol.* **10**, 6257.

[26] Ready, M. P., Kim, Y., & Robertus, J.D. (1991) *Proteins*, **10**, 270.

[27] Olson, M.A. (manuscript in preparation).

[28] Heus, H. A. & Pardi, A. (1991)*Science* **114**, 453.

BIBLIOGRAPHY/ABSTRACTS

1. *Simulation Analysis of Formycin 5'-Phosphate Analog Substrates in the Ricin A-Chain Active Site*, M. A. Olson, J. P. Scovill, & D. C. Hack (submitted to *J. Computer-Aided Molecular Design*).

2. *Molecular Dynamics Simulation of Adenyl-3',5'-Guanosine in the Ricin A-Chain Active Site*, M. A. Olson (submitted to *J. Amer. Chem. Soc.*)

CONTRACT PERSONNEL

During the contract period of 1 October 1992 thur 30 September 1993, Dr. Mark A. Olson was the sole personnel receiving pay from the contract support.